160-Gb/s NRZ-DQPSK optical transmission system employing QC-LDPC code

Sha Li (李 莎)[1*], Chongxiu Yu (余重秀)[1], Zhe Kang (康 喆)[1], Gerald Farrell[2], and Qiang Wu (吴 强)[2]

[1]*State key laboratory of Information Photonics and Optical communications, Beijing University of Posts and Telecommunications, Beijing 100086, China*

[2]*Photonic Research Centre, Dublin Institute of Technology, Dublin, Ireland*

[*]*Corresponding author: lscomeon@163.com*

Received September 30, 2013; accepted December 3, 2013; posted online January 8, 2014

A quasi-cyclic low-density parity check (QC-LDPC) code is constructed by an improved stability of the shortest cycle algorithm for 160-Gb/s non-return zero differential quadrature phase shift keying (NRZ-DQPSK) optical transmission system with the fiber-based optical parametric amplifier (FOPA). The QC-LDPC code with stability of the shortest cycle reduces the bit error ratio (BER) to 10^{-14} and restrains the error floor effectively.

OCIS codes: 060.4510, 220.4830, 190.4223.
doi: 10.3788/COL201412.010604.

Optical fiber communication systems along with optical amplifiers have many advantages, such as large capacity, distance transmission, and anti-interference. However, the dispersion effect of fiber leads to optical signal distortion, and the transmission distance is limited. With the progress of time, low-speed fiber optical network has been far from satisfying the people's requirements. High-speed and long-distance transmission fiber optical system has been put on the agenda.

In order to ensure high-speed transmission, forward error correction (FEC) coding has become an increasingly important tool and simplifies modulation devices meanwhile. Low-density parity check (LDPC) code is regarded as a superior one over many FEC codes, which has the great performance approaching the Shannon limit from with the gap just is 0.0045 dB[1,2]. The feature is very suitable for the high-speed optical fiber communication. Quasi-cyclic LDPC (QC-LDPC) code is a special code in numerous LDPC codes. However, it can be implemented just by using shift register to simplify hardware. Several QC-LDPC coding schemes have been recently presented for 100-Gb/s coherent transmission system[3−6]. Meanwhile, in order to realize long-distance transmission, optical amplifiers are adopted in optical system. Erbium-doped fiber amplifier (EDFA) is used universally in optical communication systems at present, but EDFA can only work in 1550-nm telecommunication window. Fiber-based optical parametric amplifier (FOPA) uses high nonlinearity fiber (HNLF) to obtain ultra-broad gain bandwidth and amplifies any wavelength, and the most important point is that it can realize amplification with 0 dB noise[7−9]. It is a development in the future and will replace EDFA.

It is known that cycles in the check matrix of QC-LDPC code will immensely influence decoding performance and reduce the convergence rate of algorithm. Especially abundant short cycles in check matrix will cause the error messages at nodes decoded incorrectly by iterative decoding algorithm; even more, the error messages will be spread to other nodes and lead to decoding failure[10−12]. Here, a QC-LDPC code is constructed by an improved stability of the shortest cycle algorithm for 160-Gb/s non-return zero differential quadrature phase shift keying (NRZ-DQPSK) signal optical transmission system employing FOPA as optical amplifier. In general, there are several shift values of circle permutation matrix for a specific condition, improved stability of the shortest cycle algorithm is able to select a proper shift value on the premise of ensuring stability of the shortest cycle for better decoding performance. First, a basis matrix is constructed according to improved progressive-edge-growth (IPEG) algorithm. Second, a candidate set of shift values of every circle permutation matrix is obtained according to Theorem 2.1 of Fossorier[13]. Finally, the candidate set of shift values is optimized according to the improved stability of the shortest cycle algorithm.

In 160-Gb/s NRZ-DQPSK signal optical transmission system employing FOPA, we aim to correct the error codes caused by system defects and dispersion effect, QC-LDPC code is adopted, the bit error ratio (BER) performance of optical transmission system is simulated, and the results show that QC-LDPC code constructed by improved algorithm can reduce BER to 10^{-14} and effectively restrain error floor.

QC-LDPC code is defined as a $c \times t$ compressed parity check matrix, as

$$\mathbf{H} = \begin{bmatrix} \mathbf{A}_{1,1} & \mathbf{A}_{1,2} & \cdots & \mathbf{A}_{1,t} \\ \mathbf{A}_{2,1} & \mathbf{A}_{2,2} & \cdots & \mathbf{A}_{2,t} \\ \vdots & \vdots & \ddots & \vdots \\ \mathbf{A}_{c,1} & \mathbf{A}_{c,2} & \cdots & \mathbf{A}_{c,t} \end{bmatrix}, \tag{1}$$

where $\mathbf{A}_{i,j}$ represents a circular right shift identity matrix with $p \times p$, $c = m/p$, $t = N/p$, $0 \leqslant c \leqslant t$, and N and m represent code length and parity bit length, respectively. Therefore, the parity check matrix of QC-LDPC code is $cp \times tp$.

A basis matrix can be constructed in terms of the shift

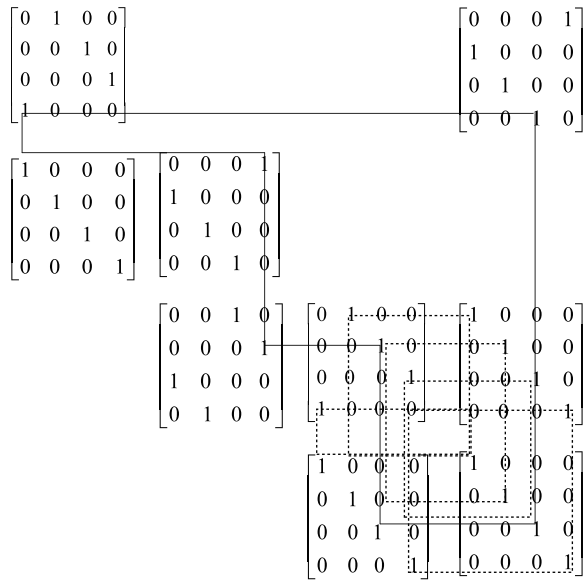

Fig. 1. Cycle of length 4 in basis matrix forms cycle of length 16 in QC-LDPC code and the cycle of length 8 in basis matrix forms cycle of length 8 in QC-LDPC code.

of the circular right shift identity matrix, as

$$\mathbf{B} = \begin{bmatrix} \mathbf{a}_{1,1} & \mathbf{a}_{1,2} & \cdots & \mathbf{a}_{1,t} \\ \mathbf{a}_{2,1} & \mathbf{a}_{2,2} & \cdots & \mathbf{a}_{2,t} \\ \vdots & \vdots & \ddots & \vdots \\ \mathbf{a}_{c,1} & \mathbf{a}_{c,2} & \cdots & \mathbf{a}_{c,t} \end{bmatrix}, \tag{2}$$

where $\mathbf{a}_{i,j} = 0$ represents unit matrix, $\mathbf{a}_{i,j} > 0$ is offset of loop transfer matrix, and $\mathbf{a}_{i,j} = -1$ is zero matrix with $p \times p$. Each column and each row of the $\mathbf{B}$ matrix represents a variable node V_i and a check node C_j, $1 \leqslant i \leqslant t$ and $1 \leqslant j \leqslant c$, respectively.

The Tanner graph of the base matrix is defined as $\mathbf{G} = (\mathbf{U} \cup \mathbf{W}, \mathbf{E})$, where $\mathbf{U} = \{V_1, K, V_t\}$ and $\mathbf{W} = \{C_1, K, C_c\}$ represent variable nodes and check nodes respectively, $\mathbf{E}$ represents a set of all the edges in Tanner graph, and e represents an edge of $\mathbf{E}$, $e = (u, c | u \in \mathbf{U}, c \in \mathbf{W}) \in \mathbf{E}$.

For example, there is a basis matrix with 0.5 code rate, $c=4$, $t=8$, and $p=4$, shift value of V_4^3 needs to be confirmed, where V_4^3 indicates the third circle permutation matrix at variable node V_4. The basis matrix is shown as

$$\mathbf{B} = \begin{array}{c} \\ C_1 \\ C_2 \\ C_3 \\ C_4 \end{array} \begin{array}{c} \begin{array}{cccccccc} V_1 & V_2 & V_3 & V_4 & V_5 & V_6 & V_7 & V_8 \end{array} \\ \begin{bmatrix} 1 & -1 & -1 & 3 & 1 & -1 & \infty & \infty \\ 0 & 3 & -1 & -1 & \infty & \infty & -1 & \infty \\ -1 & 2 & 1 & 0 & \infty & \infty & \infty & -1 \\ -1 & -1 & 0 & 1 & -1 & \infty & \infty & \infty \end{bmatrix} \end{array}. \tag{3}$$

Form Eq. (3), there are two cycles of length 4 and 8 in V_4^3

$$\begin{aligned} V_4^3(4) &= V_4 - C_4 - V_3 - C_3 - V_4, \\ V_4^3(8) &= V_4 - C_4 - V_3 - C_3 - V_2 \\ &\quad - C_2 - V_1 - C_1 - V_4, \end{aligned} \tag{4}$$

where $V_4^3(4)$ and $V_4^3(8)$ indicate cycles of length 4 and 8 in V_4^3. The candidate sets of shift value of circle permutation matrix in Eq. (4) are calculated according to the Theorem 2.1 of Fossorier,

$$\begin{aligned} N_{V_4^3}(4) &= \{0, 1, 2\}, \\ N_{V_4^3}(8) &= \{1, 2, 3\}, \end{aligned} \tag{5}$$

where $N_{V_4^3}(4)$ and $N_{V_4^3}(8)$ are the candidate sets of shift value of circle permutation matrix with cycles of length 4 and 8. The conventional algorithms only consider breaking the shortest cycle in the basis matrix when the shift value of circle permutation matrix is selected, but cannot ensure the stability of the shortest cycle maximization in QC-LDPC code matrix. If 0 is selected to be the offset in V_4^3, the cycle of length 4 will form cycle of length 16 in QC-LDPC code and the cycle of length 8 in basis matrix will form cycle of length 8 in QC-LDPC code. The shortest cycle in QC-LDPC code becomes length 8 from length 16, which influences the stability of the shortest cycle (Fig. 1).

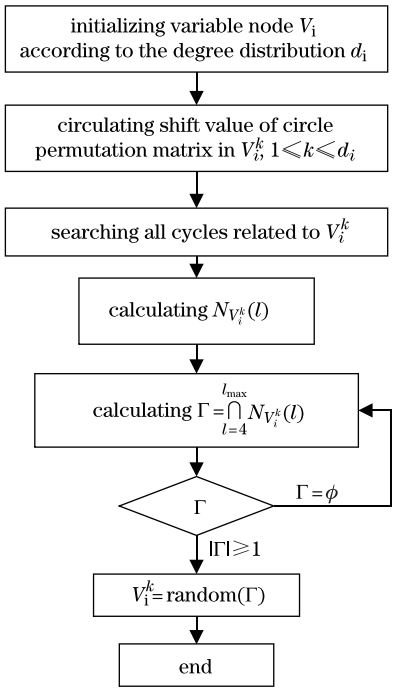

Fig. 2. Flow diagram of the stability of the shortest cycle algorithm.

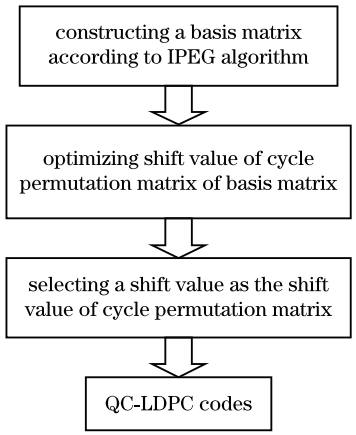

Fig. 3. Flow diagram of constructing a QC-LDPC code.

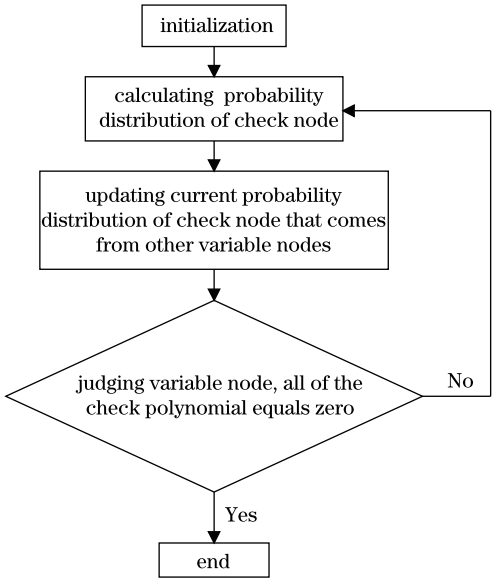

Fig. 4. Flow diagram of BP iterative decoding progress.

Improved stability of the shortest cycle algorithm can be described as shown in Fig. 2, where V_i represents the ith variable node in basis matrix, d_i is the corresponding degree distribution, V_i^k is the shift value of the kth cycle permutation matrix at V_i, random is a function that selects one from x randomly, $N_{V_i^k}(l)$ is defined as the intersection set of cycle with length l, $\mid \Gamma \mid$ indicates the number of element in Γ. According to improved stability of the shortest cycle algorithm, QC-LDPC code can be constructed as showed in Fig. 3.

QC-LDPC code is also used in belief propagation (BP) algorithm for decoding. BP algorithm is a soft-decision decoding algorithm[14]. It gets the posteriori probability through iterative operation so that the performance of QC-LDPC codes approaches the Shannon limit. BP algorithm gets the probability distribution of each node according to the updated information that is transferred between the variable nodes and check nodes in the Tanner graph. The transferred information in the Tanner graph is defined as extrinsic information. The BP iterative decoding progress is described as shown in Fig. 4.

When BP algorithm converges to the posteriori probability of all the nodes in the Tanner graph, QC-LDPC codes will have a good performance, which means that there are no cycles in the Tanner graph corresponding to the check matrix. However, the actual Tanner always includes cycles. It has proved that as long as cycles in the Tanner graph will influence on BP algorithm. The shortest cycle length is enlarged according to the improved stability of the shortest cycle algorithm that optimizes the shift value of the circle permutation matrix in the basis matrix.

System architecture of optical transmission system based on QC-LDPC code is shown in Fig. 5. The input 160-Gb/s electrical signal is first coded by a QC-LDPC coder module based on improved stability of the shortest cycle algorithm and then modulated onto an optical carrier, whose average power and central wavelength are 0.01 mW and 1 552.5 nm respectively, with DQPSK format for E/O conversion. Modulated optical signal is afterward launched into single-mode fiber (SMF) whose length is 0.625 km and attenuation is 0.24 dB/km. In order to realize long-distance transmission in SMF, the power of the output optical signal with peak power –19 dBm needs amplifying to transmit in another fiber. Because FOPA has so many advantages as mentioned before, we adopt FOPA as the system amplifier in optical transmission system. Thus, a FOPA that consists of a 50-m HNLF and one pump at 1 539 nm with peak power 30 dBm in frequency domain is selected to enhance the signal. The NL1016-B HNLF with zero-dispersion at 1 550 nm has watt profile design, introducing an inner cladding with low refractive index around step-index core, nonlinearity coefficient is 10 $W^{-1}km^{-1}$, and attenuation coefficient is 1.2 dB/km at 1 540 nm. With the action of such a parametric amplifier, a high gain with 8 dB can be no doubt obtained easily. Before amplification in the FOPA, a part of the output optical signal from the SMF is first delivered into a photoelectric detection (PD) and a phase lock loop (PLL) with a 99/1 coupler to control the phase of pump in FOPA. At the output port of HNLF, 1% optical signal is separated by another 99/1 coupler and launched into an optical spectrum analyzer (OSA) to observe the four-wave mixing (FWM) effect, while the other 99% is filtered by an optical bandpass filter (BPF) for DQPSK optical demodulation module. Demodulated electrical signal with error bits is finally QC-LDPC decoded and used for recovery of original signal.

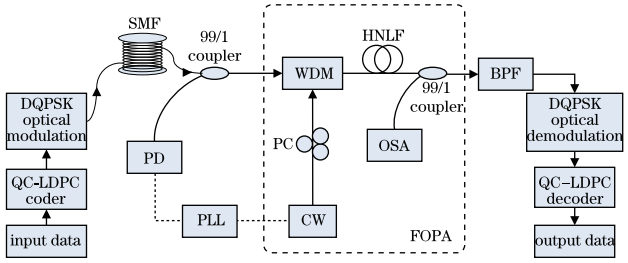

Fig. 5. 160-Gb/s NRZ-DQPSK signal transmission system employing QC-LDPC code. CW, continuous wave laser; PC, polarization controller; WDM, wavelength division multiplexing.

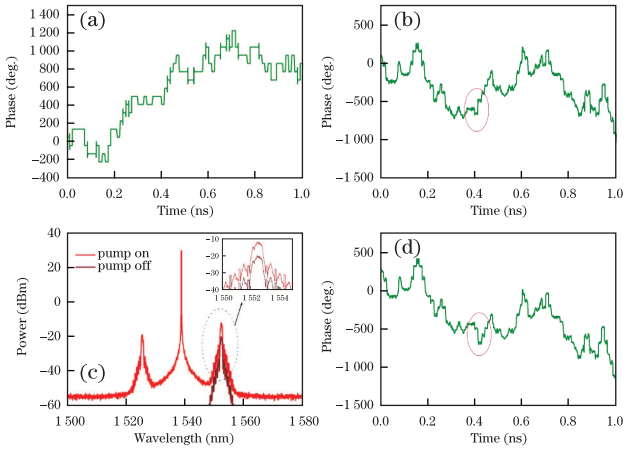

Fig. 6. (a) Segment phase of 160-Gb/s QC-LDPC code signal after DQPSK optical modulation module. (b) A segment phase of optical carrier after SMF. (c) FWM spectrum after FOPA. (d) A segment phase of amplified optical signal after BPF.

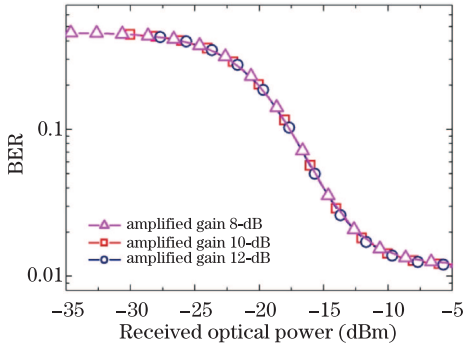

Fig. 7. BER versus received optical power with different amplification gain after DQPSK optical demodulation module.

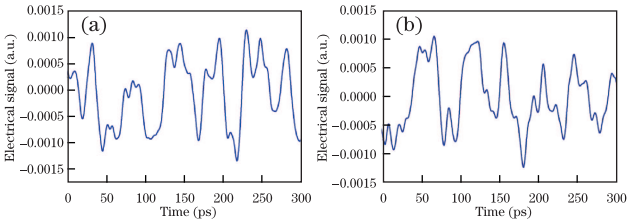

Fig. 8. Demodulation electrical signal at (a) I and (b) Q branches. The inset shows eye diagram.

First, 2040, 2720, and 3400 pseudo-random codes with 160-Gb/s speed are fed into the system as the input data, respectively. The pseudo-random codes are coded by the improved stability of the shortest cycle algorithm to QC-LDPC code with different redundancy rates 50%, 33%, and 16% respectively and the QC-LDPC code length is 4080. The signal is detected at several points and is analyzed. Figure 6(a) shows a segment phase of 160-Gb/s QC-LDPC code signal after DQPSK optical modulation module; the data are carried on relative phase of optical carrier. When optical signal transfers in SMF, it will be distorted by dispersion, attenuation, and nonlinearity. A segment phase of optical carrier is shown in Fig. 6(b); there is a drastic random jitter on the phase of optical signal. After FOPA, the FWM spectrum is shown in Fig. 6(c), the attenuation optical signal is amplified about 8 dB. Then, a bandpass filter with center wavelength at 1 552.5 nm is used to slice the amplified signal; a segment phase of amplified optical signal is shown in Fig. 6(d). However, the amplification process is not ideal and pump jitter and phase mismatch will distort transmission optical signal; the differences are shown in Figs. 6(b) and (d) with a red circle. Actually, bit error from FOPA can be neglected relative to one from fiber. When the amplification gain is adjusted, the BER does not move after DQPSK demodulation module, as shown in Fig. 7.

In DQPSK demodulation module, demodulation electrical signals are detected at I and Q branches as shown in Figs. 8(a) and (b); the inset shows eye diagrams. Electrical signals have serious random jitter, high BER will be brought not using QC-LDPC decoder.

In 160-Gb/s NRZ-DQPSK optical transmission system based on QC-LDPC codes with different redundancy rates, basis matrixes are 12×24, 8×24, and 4×24, respectively; cycle transfer matrix is $p = 170$; the shortest cycle lengths are g=8, 8, and 6, respectively. After QC-LDPC decoder, the results of simulations are shown in Fig. 9, for nonlinearity, dispersion, attenuation from fiber and pump jitter, and phase mismatch from FOPA are considered. If OOK modulation format is used, BER almost equals to 1 and the modulation does not adapt to high-speed optical transmission system. If DPSK modulation format is used, the BER becomes smaller than the one using OOK modulation and is 0.1 at the error floor. When DQPSK modulation format is adopted, BER is the smallest among three modulation formats. It is not advisable that only modulation format is changed to obtain low BER in optical transmission system, transmitting and receiving equipment will become complication and be difficult to control. Under conditions of DQPSK modulation format, QC-LDPC code is used to reduce BER and restrain error floor. As shown in Fig. 9, we test QC-LDPC codes of different redundancy rates; QC-LDPC(4080,2040) code of 50% redundancy rate significantly outperforms the other two codes. At a BER of 3.52×10^{-12}, the QC-LDPC code of redundancy rate 16% is 3.8 dB away from the one of redundancy rate 33%, while at a BER of 1.66×10^{-13}, the QC-LDPC code of redundancy rate 33% is 2.56 dB close to the one of redundancy rate 50%. Although we do not possess the results of simulations at 10^{-15}, the QC-LDPC code is constructed by the proposed improved stability of the shortest cycle algorithm do not exhibit error floor.

In conclusion, we propose an improved stability of the shortest cycle algorithm to construct QC-LDPC code and investigate its performance. The QC-LDPC code constructed by improved stability of the shortest cycle algorithm effectively corrects error bits caused by nonlinearity, dispersion and pump jitter, and phase mismatch in the optical transmission system. A BER of 10^{-14} at the received optical power of –23.55 dBm is achieved. Moreover, this proposed QC-LDPC code, since it ensures stability of the shortest cycle, is expected to inherently enable efficient high-speed implementation. Our approach, thus, provides a promising solution for 160 Gb/s and beyond.

This work was supported by the National "973" Program of China (Nos. 2010CB327605 and 2010CB328304), the Key Grant of Ministry of Education of China (No. 109015), the Program for New Century Excellent Talents in University (No. NECT-11-0596), the Beijing Nova Program (No. 2011066), the

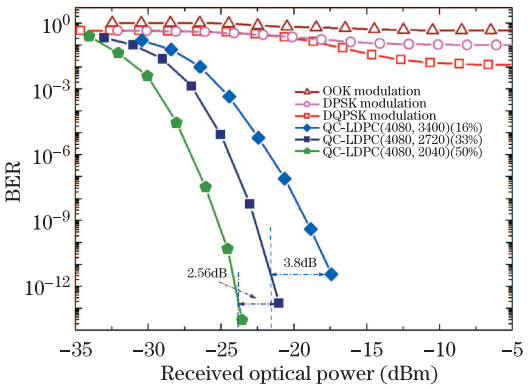

Fig. 9. BER versus received optical power after QC-LDPC decoder.

Specialized Research Fund for the Doctoral Program of Higher Education (No. 20120005120021), the Fundamental Research Funds for the Central Universities (No. 2013RC1202), the China Postdoctoral Science Foundation (No. 2012M511826), and the Postdoctoral Science Foundation of Guangdong Province (No. 244331).

References

1. S. Y. Chung, G. D. Forney Jr., T. J. Richardson, and R. Urbanke, Commun. Lett. **5,** 58 (2001).
2. P. Venkateshwari and M. Anbuselvi, in *Proceedings of ICRTIT 2012* 292 (2012).
3. N. Kamiya and S. Shioiri, in *Proceedings of OSA/OFC/NFOEC 2010* OThL2 (2010).
4. D. Chang, F. Yu, Z. Xiao, and Y. Li, in *Proceedings of OSA/OFC/NFOEC 2011* OTuN2 (2011).
5. S. Zou, Y. Wang, Y. Shao, J. Zhang, J. Yu, and N. Chi, Chin. Opt. Lett. **10,** 070605 (2012).
6. C. Zhang, L. Chai, Y. Song, M. Hu, and C. Wang, Chin. Opt. Lett. **11,** 051403 (2013).
7. J. Hansryd and P. A. Andrekson, IEEE J. Sel. Top. Quantum Electron. **8,** 506 (2002).
8. R. M. Jopson and A. H. Gnauck, in *Proceedings of OECC 2012* 59 (2012).
9. P. A. Andrekson, in *Proceedings of OFC/NFOEC* OM3B.6 (2012).
10. H. Xiao and A. H. Banihashemi, Commun. Lett. **8,** 715 (2004).
11. S.-H. Kim., Commun. Lett. **7,** 607 (2007).
12. C. T. Healy and R. C. de Lamare, Commun. Lett. **16,** 889 (2012).
13. M. P. C. Fossorier, IEEE Trans. Inform. Theor. **50,** 1788 (2004).
14. Y. Wu, A. Yang, Y. Sun, and Q. Zhao. Chin. Opt. Lett. **10,** S10605 (2012).